ANALYSIS OF A CORNER LAYER PROBLEM IN ANISOTROPIC INTERFACES

N.D. ALIKAKOS, P.W. BATES, J.W. CAHN, P.C. FIFE, G. FUSCO, AND G.B. TANOGLU

Abstract. We investigate a model of anisotropic diffuse interfaces in ordered FCC crystals introduced recently by Braun et al and Tanoglu et al [BCMcFW, T, TBCMcF], focusing on parametric conditions which give extreme anisotropy. For a reduced model, we prove existence and stability of plane wave solutions connecting the disordered FCC state with the ordered Cu_3Au state described by solutions to a system of three equations. These plane wave solutions correspond to planar interfaces. Different orientations of the planes in relation to the crystal axes give rise to different surface energies. Guided by previous work based on numerics and formal asymptotics, we reduce this problem in the six dimensional phase space of the system to a two dimensional phase space by taking advantage of the symmetries of the crystal and restricting attention to solutions with corresponding symmetries. For this reduced problem a standing wave solution is constructed that corresponds to a transition that, in the extreme anisotropy limit, is continuous but not differentiable. We also investigate the stability of the constructed solution by studying the eigenvalue problem for the linearized equation. We find that although the transition is stable, there is a growing number $0(\frac{1}{\epsilon})$, of critical eigenvalues, where $\frac{1}{\epsilon} \gg 1$ is a measure of the anisotropy. Specifically we obtain a discrete spectrum with eigenvalues $\lambda_n = \epsilon^{2/3}\mu_n$ with $\mu_n \sim Cn^{2/3}$, as $n \to +\infty$. The scaling characteristics of the critical spectrum suggest a previously unknown microstructural instability.

Key words: Singular perturbations, connecting orbits, anisotropy, diffuse interfaces, face-centered cubic crystals, microstructures.

1. Introduction

The motivation for this paper is the study of properties of phase interfaces in alloys. These interfaces are realized as grain boundaries. Increasingly popular approaches to modeling the complex physics of such interfaces are found in phase field theories, in which order parameters of various kinds are used as pointwise descriptors of salient material properties, on both the microscale and mesoscale levels. The order parameters have specific values in pure phases, but are not restricted to discrete values; rather they vary continuously from one phase to another in thin interphase regions. Although most modeling in the past has utilized a single rather vaguely defined order parameter in this description, it has been shown (e.g. [NC, BCMcFW] that multiple order parameter formulations can be used to reflect the basic crystallography of the material in a more natural manner. In particular, given a specific lattice, explicit definitions of these parameters can be given in terms of local averages of the populations of atomic species at the sites on sublattices.

In this vein, our starting point is the multiple-order-parameter description of some FCC crystals given by Braun et al [BCMcFW]. Their phase-field model leads to a system of

NDA supported by grants from the University of North Texas and the University of Athens. PWB supported by NSF DMS 9970894 and NSF DMS 0200961.

second order ordinary differential equations for the variation of the order parameters, hence of various other properties, across a stationary planar interface. The independent variable is a spatial coordinate normal to the interface. Extracting information analytically from such systems is far more difficult than it is for the much more prevalent single-order-parameter models found in the literature.

Nevertheless, important qualitative information can be obtained in special cases. In particular, the size of the system of equations can be reduced if certain symmetries are assumed and the orientation of the interface relative to that of the crystal axes is compatible with those symmetries. We make these assumptions in the present paper, and in addition consider formal reductions related to the anisotropy of the alloy being high.

These conditions reduce the interface problem to a singularly perturbed pair of second order ODE's with limiting conditions at $\pm\infty$. There is a base (singular limit) solution, easily found, forming a formal approximation to the exact solution in most of its domain. The unusual feature of this base solution is the fact that it has a singularity in the interior of its domain. At the singularity, which is pitchfork type, the base solution is continuous but not differentiable. The presence of this singularity is what makes this a singular perturbation problem; not the presence of boundary layers, which often (but not in this case) accompany solutions when a small parameter multiplies a higher derivative.

This singularity is a source of mathematical interest as well as of difficulty. In a small neighborhood of it, the variables may be rescaled to create a "corner layer" representation of the solution in the form of a boundary value problem on an infinite interval. Our focus is on the existence and stability (in a spectral sense) of a solution to this BVP. The existence and spectral results are stated in Sec. 3, and their proofs are in Sec. 4. Preliminary considerations are developed in Sec. 2. The rest of Sec. 1 is devoted to constructing the model from the materials scientific setting.

1.1. **The Model.** We will be dealing with 3D lattices, and with a type of crystal known as FCC (face-centered cubic). Quite analogous problems and methods hold for other structures; for example in the case of crystals of the hexagon-closely-packed type the analogy is almost complete. The FCC is a periodic arrangement of atoms whose unit cell is a cube with atoms occupying its corners and the centers of its faces. We can identify 3 distinguished planar cuts intersecting at least four lattice points in a unit cell, corresponding to the normal directions $\overline{n} = \left(\frac{1}{\sqrt{3}}, \frac{1}{\sqrt{3}}, \frac{1}{\sqrt{3}}\right)$, $\overline{n} = (1, 0, 0)$, $\overline{n} = \left(0, \frac{1}{\sqrt{2}}, \frac{1}{\sqrt{2}}\right)$, with reference to the coordinates ξ_i shown in Fig. 1.

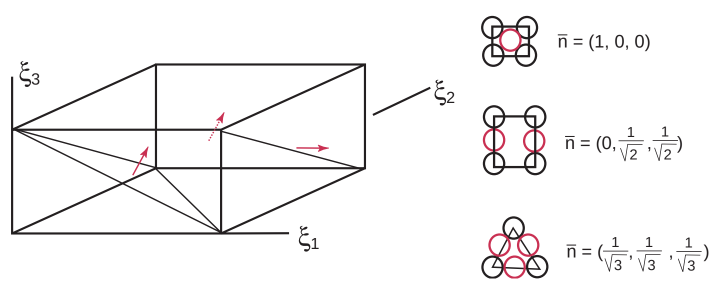

FIGURE 1. The distinguished planar cuts. The ξ_i are spatial coordinates aligned with the crystal.

Each unit cell in the FCC contains the equivalent of 4 whole atoms and a tetrahedron can be associated with it, as shown in Fig. 2. Each numbered point of such a tetrahedron can serve as the origin of a primitive cubic Bravais sublattice. The FCC lattice then is decomposed into 4 numbered sublattices.

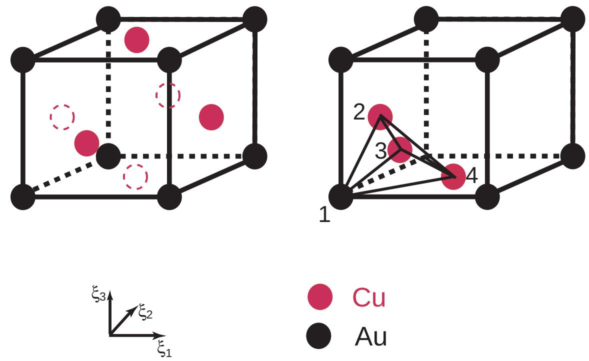

FIGURE 2. A unit cell of the FCC lattice, and the tetrahedron whose corners serve to number the four primitive cubic sublattices.

Following [BCMcFW], in our work we will consider, as a specific illustrative prototype, the alloy Cu_3Au, so that each lattice site is occupied by either a Cu or Au atom, and we will focus in this paper on order-disorder transitions and the associated interphase boundaries. In the ordered form of the alloy, the copper atoms occupy the centers of the faces and the gold atoms lie on the vertices. Four numbers $\rho_1, \rho_2, \rho_3, \rho_4$ are defined (when ordering is allowed to be imperfect) to be the fraction of atoms on each primitive cubic sublattice which are Cu. When ordering is perfect, copper represents $\frac{3}{4}$ of the total. Hence for the ordered Cu_3Au state,

$$\rho_1(\text{ord}) = 0, \;\; \rho_2(\text{ord}) = \rho_3(\text{ord}) = \rho_4(\text{ord}) = 1,$$

while for the disordered state the locations of the Cu atoms are random, given the total density, so that

$$\rho_1(\text{dis}) = \rho_2(\text{dis}) = \rho_3(\text{dis}) = \rho_4(\text{dis}) = \frac{3}{4}.$$

In our treatment, the order parameters ρ_i are taken to vary continuously within the order-disorder transition region. The equations we will be dealing with are written in terms of the alternative variables X, Y, Z, W, defined as linear combinations of the ρ's:

$$\begin{aligned} X &= -\rho_1 - \rho_2 + \rho_3 + \rho_4, \\ Y &= -\rho_1 + \rho_2 - \rho_3 + \rho_4, \\ Z &= -\rho_1 + \rho_2 + \rho_3 - \rho_4, \\ W &= \tfrac{1}{4}(\rho_1 + \rho_2 + \rho_3 + \rho_4). \end{aligned} \tag{1}$$

The intuition behind this transformation is that the new order parameters are more amenable to continuizing [NC]. The first three are nonconserved order parameters and the fourth, W, is conserved, since it represents the total density of copper in the crystal. It will be taken as fixed (in a more complete model, W would be taken as fixed not pointwise, but only on the average [T]). The disordered and ordered states correspond to

$$X = Y = Z = 0 \text{ and } X = Y = Z = 1, \text{ respectively.}$$

Since W is held fixed, the free energy function used in [BCMcFW] depends only on $X,\ Y,\ Z$ and their gradients:

$$J(X,Y,Z)=\int_V [Q(\nabla X,\nabla Y,\nabla Z)+F(X,Y,Z)]\,d\xi_1 d\xi_2 d\xi_3, \tag{2}$$

where the space coordinates are (ξ_1,ξ_2,ξ_3) and V is the volume occupied by the sample.

Here Q is a positive definite quadratic form; its presence in the free energy expression reflects a proclivity of material phases to be uniform. It also accounts for interfacial surface tension, and the anisotropy of this tension, reflected through the different coefficients of Q, will play a considerable role in the model.

The bulk free energy function F is a fourth degree polynomial which is positive except at its several global minima, including $(0,0,0)$ and $(1,1,1)$. A specific polynomial, given below, will be used in our model as representative of any function with that property. It will be specified that $F(0,0,0)=F(1,1,1)$. To represent real alloys, the coefficients of F would depend on temperature; this constraint is then a statement that the temperature will be at the transition value for order-disorder transitions.

The gradient terms Q are taken to be of the form $Q=AQ_1+BQ_2$, where Q_i are simple sums of squares of derivatives. Since Q_1 is isotropic, the ratio B/A measures the degree of anisotropy of the free energy. We use the explicit expressions

$$F(X,Y,Z)=2(X^2+Y^2+Z^2)-12XYZ+(X^4+Y^4+Z^4)+(X^2Y^2+X^2Z^2+Y^2Z^2), \tag{3}$$

$$\begin{aligned} Q_1&=\tfrac{1}{2}\left[\left(\tfrac{\partial X}{\partial\xi_1}\right)^2+\left(\tfrac{\partial Y}{\partial\xi_2}\right)^2+\left(\tfrac{\partial Z}{\partial\xi_3}\right)^2\right],\\ Q_2&=\tfrac{1}{2}\left[\left(\tfrac{\partial X}{\partial\xi_2}\right)^2+\left(\tfrac{\partial X}{\partial\xi_3}\right)^2+\left(\tfrac{\partial Y}{\partial\xi_1}\right)^2+\left(\tfrac{\partial Y}{\partial\xi_3}\right)^2+\left(\tfrac{\partial Z}{\partial\xi_1}\right)^2+\left(\tfrac{\partial Z}{\partial\xi_2}\right)^2\right]. \end{aligned} \tag{4}$$

The truncation to fourth degree is discussed in [BCMcFW] and the extension to sixth degree in [T]. The inclusion of cubic terms is sufficient for the existence of first-order transitions.

The governing evolution PDE's in a phase-field theory are given by the L^2 gradient flow of the functional J:

$$\tau\frac{\partial}{\partial t}\begin{pmatrix}X\\Y\\Z\end{pmatrix}=L\begin{pmatrix}X\\Y\\Z\end{pmatrix}-\nabla F(X,Y,Z), \tag{5}$$

where L is a diagonal matrix of second degree elliptic operators in the space variables, and ∇ denotes the gradient with respect to the variables (X,Y,Z), and τ is a dimensionless relaxation time.

Although we have described the model in terms of the ordering of a binary alloy, important features carry over in some cases to analogous models for the solidification of a pure material.

The fundamental paper [BCMcFW] contains, in addition to the derivation of the model, a bifurcation analysis of the uniform steady states, numerical and formal asymptotic analyses of plane wave solutions for large anisotropy ratios $B/A\equiv\epsilon^{-2}$, and numerical calculation of the Wulff shapes. This paper together with [T] are our basic references. Other related work is cited in these references. We remark that the parameter ϵ should not be confused with the usual epsilon appearing before the gradient in the Allen-Cahn and Cahn-Hilliard equations, where it has an entirely different meaning.

Plane waves in the direction $\overline{n}$ and velocity V are solutions of (5) of the form

$$X = x(\overline{n}\cdot(\xi_1,\xi_2,\xi_3) - Vt) = x(\zeta),\ Y = y(\zeta),\ Z = z(\zeta). \tag{6}$$

With boundary conditions $x(-\infty) = y(-\infty) = z(-\infty) = 0,\ x(\infty) = y(\infty) = z(\infty) = 1$, they represent planar interfaces with normal $\overline{n}$ separating an ordered state from a disordered state. The functions $\overline{x} = (x, y, z)$ satisfy (derivatives are with respect to ζ)

$$-V\overline{x}' = \Lambda\overline{x}'' - \nabla F(x, y, z), \tag{7}$$

where Λ is a diagonal matrix whose elements are linear functions of A and B, and quadratic functions of $\overline{n}$.

Recall that the temperature has been chosen so that $F(0, 0, 0) = F(1, 1, 1)$. This a priori implies that $V = 0$.

1.2. **Reductions.** Simplifications to the system (7) can be made by seeking only those profiles which satisfy certain symmetry constraints. Of course the direction $\overline{n}$ must be chosen so that the resulting profile satisfies those constraints, and the function F and the matrix Λ have to be compatible with them as well.

One such possible constraint is the restriction of the order parameters to the plane $Y = Z$ (hence $y = z$). In the crystal, this is tied to the symmetry between two sites on the elementary tetrahedron. Note from (1) that $Y = Z \Rightarrow \rho_3 = \rho_4$ and that the two symmetric sites share the same ξ_1 coordinate. Therefore if we take $\overline{n}$ so that $n_2 = n_3$, the symmetry $Y = Z$ should be preserved through the transition. This is indeed true. To exhibit the resulting system, we define our anisotropy parameter

$$\epsilon = \sqrt{A/B}, \tag{8}$$

the reduced free energy $G(X, Y) = F(X, \frac{1}{\sqrt{2}}Y, \frac{1}{\sqrt{2}}Y)$ (this effectively changes the physical meaning of Y) and an angle α. This angle is given by $\overline{n} = (\cos\alpha, \frac{1}{\sqrt{2}}\sin\alpha, \frac{1}{\sqrt{2}}\sin\alpha)$, $0 \leq \alpha \leq \pi$, Then (7) is reduced to

$$\begin{aligned} &(\cos^2\alpha + \epsilon^2\sin^2\alpha)x'' - G_x(x, y) = 0,\ x(-\infty) = y(-\infty) = 0, \\ &(\epsilon^2\cos^2\alpha + \tfrac{1+\epsilon^2}{2}\sin^2\alpha)y'' - G_y(x, y) = 0,\ x(\infty) = 1, y(\infty) = \sqrt{2}. \end{aligned} \tag{9}$$

The special cases $\alpha = 0$ and $\alpha = \pi/2$ correspond to the distinguished cuts $(1, 0, 0)$ and $(0, \frac{1}{\sqrt{2}}, \frac{1}{\sqrt{2}})$ already mentioned above. When $\epsilon \ll 1$, the problem for the profile at $\alpha = 0$ or $\alpha = \pi/2$ can be considered to be a difficult perturbation problem from a limit profile at $\epsilon = 0$. In the case $\alpha = 0$, the problem is particularly difficult because of a degeneracy (irregularity) in the limit profile which does not allow for the application of the Fenichel theory with its variants and extensions [J].

The $(1, 0, 0)$ direction is especially significant because evidence suggests it may be the direction that globally minimizes interfacial energy. In this case the system (9) (with $V = 0$) takes the form

$$\left\{ \begin{array}{l} x'' = G_x(x,y) \\ \epsilon^2 y'' = G_y(x,y) \end{array} \right. \iff \left\{ \begin{array}{l} u_1' = u_2 \\ u_2' = G_x(u_1,u_3) \\ \epsilon u_3' = u_4 \\ \epsilon u_4' = G_y(u_1,u_3) \end{array} \right. \tag{10}$$

via the change of variables $u_1 = x$, $u_2 = x'$, $u_3 = y$, $u_4 = \epsilon y'$. The resulting first order system is Hamiltonian. The limiting system at $\epsilon = 0$ is

$$\left\{ \begin{array}{l} u_1' = u_2 \\ u_2' = G_x(u_1,u_3) \\ 0 = u_4 \\ 0 = G_y(u_1,u_3). \end{array} \right. \tag{11}$$

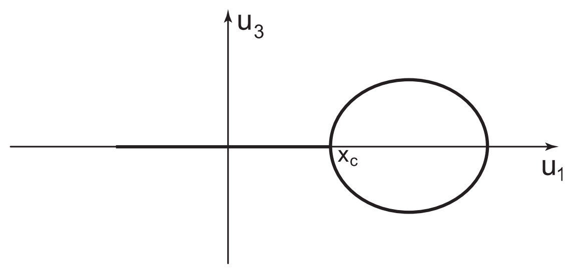

FIGURE 3. The projection of the set $M_0 = \{(u_1,u_2,u_3,u_4)\,|u_4 = 0, G_y(u_1,u_3) = 0\}$ on the $u_1 - u_3$ plane. The horizontal part together with the upper branch constitute the graph of h (see (15)). The choice of the lower branch leads to analogous results.

The main point of mathematical interest is a difficulty which stems from the fact that the limit manifold of critical points $M_0 = \{u_4 = 0,\ G_y(u_1,u_3) = 0\}$ is not smooth at a value $x = X_c$ (see Fig. 3). We stress that this is not just a technicality. The singularity encodes the physics of the transition. It turns out that the mathematical structure is completely different from that in the $(0, \frac{1}{\sqrt{2}}, \frac{1}{\sqrt{2}})$ direction which fits more or less in the framework of [Fe, J]. For this case we refer the reader to [S, AFFS].

We note that the results in this paper have only suggestive value for the system (9), $\alpha = 0$, since the reductions to follow, though well motivated, are very formal.

2. Geometric and algebraic characteristics of G

We begin with (10):

$$\left\{ \begin{array}{ll} \dfrac{d^2x}{d\zeta^2} - G_X(x,y) = 0, & x(-\infty) = 0,\ x(+\infty) = 1, \\ \\ \varepsilon^2\, \dfrac{d^2y}{d\zeta^2} - G_Y(x,y) = 0, & y(-\infty) = 0,\ y(+\infty) = \sqrt{2}, \end{array} \right. \tag{12}$$

where

$$G(X,Y) = 2(X^2+Y^2) - 6XY^2 + X^2Y^2 + X^4 + \frac{3}{4}Y^4. \tag{13}$$

We determine the critical points of G:

(i) $G_X(X,Y) = 0 \Leftrightarrow 4X - 6Y^2 + 4X^3 + 2XY^2 = 0$

(ii) $G_Y(X,Y) = 0 \Leftrightarrow 2Y(2 - 6X + X^2 + \frac{3}{2}Y^2) = 0.$

From (ii) we obtain

$$Y = 0 \quad \text{or} \quad Y = \pm\sqrt{2}\, h(X), \tag{14}$$

$$h(X) = \begin{cases} 0, \;\; X < X_c = 3 - \sqrt{7} \cong 0.35, & \text{where } \; 2 - 6X_c + X_c^2 = 0 \\[2ex] h_0(X) = \left(-\dfrac{X^2 - 6X + 2}{3}\right)^{\frac{1}{2}}, & X_c \le X \le 1. \end{cases} \tag{15}$$

Substituting in (i) we obtain

$$4X - 12h^2(X) + 4X^3 + 4Xh^2(X) = 0. \tag{16}$$

Further calculations finally yield the critical points

$$\begin{cases} (0,0), \;\; (1, \pm\sqrt{2}), & \text{global minimizers of } \; G, \\[2ex] \left(\dfrac{1}{2}, \pm\sqrt{2}\; h\!\left(\dfrac{1}{2}\right)\right) & \text{saddle points.} \end{cases} \tag{17}$$

Notice that $0 < X_c < \frac{1}{2}$.

There is a useful mechanical analog to (12). We think of ζ as time and system (12) as the Newton equations describing a ball rolling in a "potential well" -G of very small inertia in the Y direction and unit inertia in the X direction. The specific connection we are constructing corresponds to a motion which for $\zeta \to \pm\infty$ is asymptotic to the two equal maxima $(0,0), (1,\sqrt{2})$ of the potential energy $-G$ (Fig. 4B). The path that the ball follows (see discussion that follows), to the first approximation when projected on the (x,y) plane, consists of $(0,0)$, the part of the x-axis up to X_c, and the upper branch up to $(1,\sqrt{2})$.

We note that

$$\begin{pmatrix} G_{XX} & G_{XY} \\ G_{YX} & G_{YY} \end{pmatrix}\Bigg|_{(X_c,0)} = \begin{pmatrix} 4 + 12X_c^2 & 0 \\ 0 & 0 \end{pmatrix}$$

from which we conclude that the G-surface is very flat near $(X_c, 0)$. In fact the principal curvature in the Y-direction vanishes. This together with the small inertia of the ball in the Y-direction suggests the possibility of an oscillatory behavior near $(X_c, 0)$. This intuition motivates our eigenvalue analysis in Theorem 2 below.

The expansion of G near $(X_c, 0)$ is:

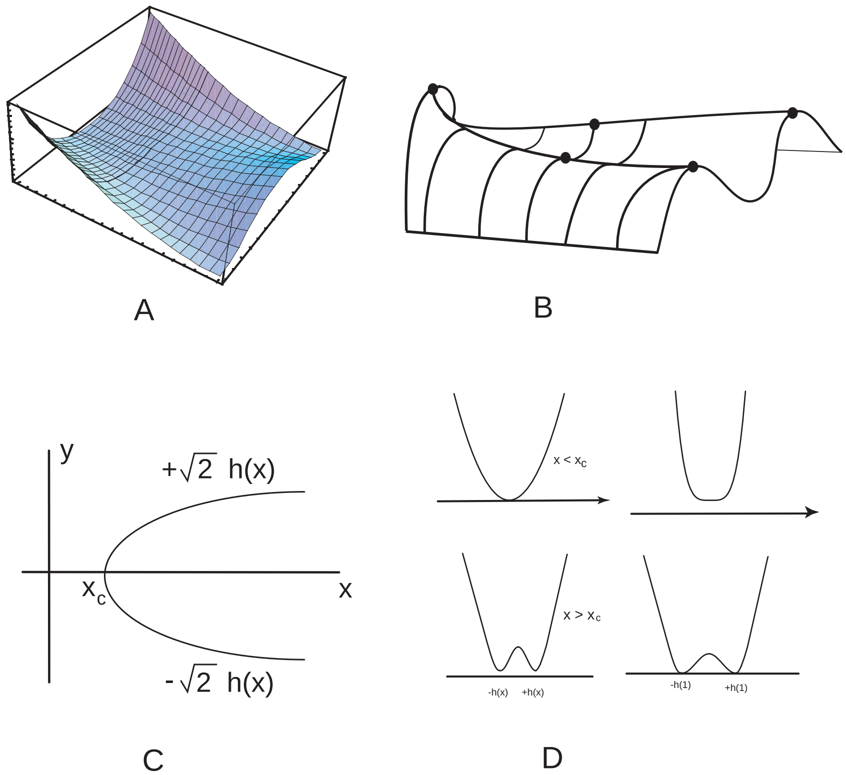

FIGURE 4. Aspects of the G-surface. (A) G as a function of X and Y. (B) The graph of $-G$. (C) Part of the level set $G_Y(X,Y)=0$. (D) G as a function of Y for various X.

$$
\begin{aligned}
G_Y(X,Y) &= 2Y\left[\frac{3}{2}Y^2 + X^2 - 6X + 2\right] \\
&= 2Y\left[\frac{3}{2}Y^2 + (2X_c - 6)(X - X_c) + O((X-X_c)^2)\right] \\
&= 2Y\left\{\left[aY^2 - b(X - X_c)\right] + O((X-X_c)^2)\right\},
\end{aligned}
\tag{18}
$$

where $a = \frac{3}{2}and \quad b = 6 - 2X_c > 0$.

Now $(12)_{(ii)}$ near X_c is approximated[1] by

$$
\epsilon^2 \frac{d^2 y}{d\zeta^2} - 2y[ay^2 - b(x - X_c)] = 0. \tag{19}
$$

Note that (12) is translation invariant. We can therefore require that

$$
x(0) = X_c. \tag{20}
$$

[1]We refer the reader to [BCMcFW] for a treatment of formal asymptotics that has motivated much of our work.

By $(12)_{(i)}$, the function $x(\zeta)$ has second derivative bounded independently of ϵ, so that near $\zeta = 0$ it may be approximated by

$$x(\zeta) \sim X_c + m\zeta, \;\; m = x'(0). \tag{21}$$

Consequently in the transition layer equation (19) can be approximated by

$$\epsilon^2 \frac{d^2 y}{d\zeta^2} - 2y[ay^2 - bm\zeta] = 0. \tag{22}$$

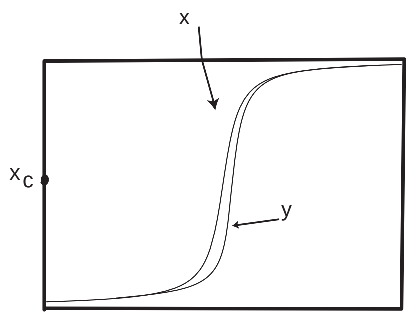

FIGURE 5. The variation of $x(\zeta)$ and $y(\zeta)$ in the layer (see [BCMcFW]). This provided the motivation for using x as the independent variable in the layer and thus reducing (12) to a single equation.

Next, following [BCMcFW], we introduce the change of variables

$$s = \frac{\zeta}{\epsilon^{2/3}}, \;\; y(\zeta) = \epsilon^{1/3} R\left(\frac{\zeta}{\epsilon^{2/3}}\right). \tag{23}$$

A computation shows that

$$R'' - 2R[aR^2 - bms] = 0, \tag{24}$$

where $''$ stands for $\frac{d^2}{ds^2}$, $s \in \mathbb{R}$.

Finally we need to motivate the boundary conditions. Recall that to first approximation the graph of the solution of (10) coincides with the x-axis from $(0,0)$ to $(X_c, 0)$ and with $y = \sqrt{2}h(x)$ for $X_c \leq x \leq 1$. Therefore near $X = X_c$, $R^2 = \frac{bm}{a}s$, and so it is natural to append to (24) the conditions

$$\begin{cases} R(s) {\rightarrow} 0 \text{ as } s {\rightarrow} -\infty, \\ R(s) = \sqrt{\frac{bm}{a}s}\,(1 + o(1)) \text{ as } s {\rightarrow} \infty. \end{cases} \tag{25}$$

In fact, it will be shown that there is a solution satisfying stronger asymptotic conditions than these.

Eq. (24), with conditions (25), describes the interior layer of the order-disorder transition, in blown-up variables (Fig. 6).

The eigenvalue problem associated with the linearization of (24) is

$$V'' - 2[3aR^2(s) - bms]V = -\mu V \text{ on } L^2(\mathbb{R}). \tag{26}$$

3. Statement of the main results

Theorem 1. *(Existence) There is a strictly increasing solution $R(s)$ of (24) satisfying*

$$\left\{\begin{array}{l} R(s) = O\left(e^s\right) \ \ \text{as } s \to -\infty, \\ \frac{R(s)}{\sqrt{\frac{bm}{a}s}} = 1 + O\left(\frac{1}{s}\right) \ \ \text{as } s \to \infty. \end{array}\right. \tag{27}$$

Theorem 2. *(The spectrum) The spectrum of (26) is discrete, simple, and positive, and*

$$0 < \mu_1 < \mu_2 < \ldots < \mu_n < \ldots, \tag{28}$$

with μ_n satisfying

$$\mu_n = \left[2bm\left(n + \frac{1}{2}\right)\pi\right]^{2/3} \quad \text{as } n \to \infty. \tag{29}$$

The corresponding eigenfunctions have nodal structure and satisfy the estimates as $n \to \infty$

$$\left\{\begin{array}{l} V_n(s) \sim c_n \mathrm{Ai}\left((4bm)^{1/2}\left(s - \frac{\mu_n}{4bm}\right)\right), \ \ s \geq K > 0, \\ V_n(s) \sim d_n \mathrm{Ai}\left((2bm)^{1/2}\left(-s - \frac{\mu_n}{2bm}\right)\right), \ \ s \leq -K < 0, \end{array}\right. \tag{30}$$

where $\mathrm{Ai}(s)$ is the Airy function, and $K > 0$ is fixed, uniform in n. Under the normalization $\int_{\mathbb{R}} |V_n(s)|^2 ds = 1$, we have the uniform estimate

$$|V_n(s)| < Const.\ n^{-1/6}. \tag{31}$$

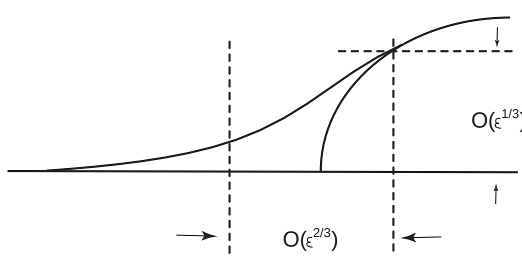

Figure 6. The solution $y(\zeta)$ in the corner layer.

Remarks

(1) Utilizing the estimate (27), we obtain that

$$2[3aR^2 - bms] \to \left\{\begin{array}{l} 4bm|s|, \ \ s \to \infty, \\ 2bm|s|, \ \ s \to -\infty. \end{array}\right.$$

In Fig. 7, we draw a typical eigenfunction of the related eigenvalue problem

$$\Psi_n'' - |s|\Psi_n = \nu_n \Psi_n, \tag{32}$$

which if rescaled appropriately, resembles $V_n(s)$ outside some fixed set $\{|s| \leq K\}$ with K independent of n.

(2) The eigenvalue problem in the original variables is

$$\epsilon^2 \frac{d^2 v}{d\zeta^2} - 2v[3ay^2 - bm\zeta] = -\lambda v \text{ on } L^2(\mathbb{R}). \tag{33}$$

Rescaling according to (23) and setting $v(\zeta) = V\left(\frac{\zeta}{\epsilon^{2/3}}\right) = V(s)$, we obtain

$$V'' - 2[3aR^2 - bms]V = -\frac{\lambda}{\epsilon^{2/3}}V.$$

Thus the relationship with (26) is $\frac{\lambda_n}{\epsilon^{2/3}} = \mu_n$. Using (29), we see that $\lambda_n \sim (n\epsilon)^{2/3}$. Thus there are $O(\epsilon^{-1})$ critical (small) eigenvalues, all of them on the stable side. It is useful to note the differences with the spectrum for the bistable nonlinearity [AMP]. Notice also that from (30) and Fig. 6 we see that the oscillations of the eigenfunctions take place in the layer.

(3) Theorem 2 establishes a type of stability of the solution, although its value is only suggestive since stability, as everything else in this paper, has to be considered in the context of the full system. The existence of a growing number of small eigenvalues, although on the stable side, suggests a certain type of instability of the interface. We believe that this behavior is related to the wetting by a differently ordered phase $L1_0$ as found in [KC] in their lattice model, and expect Thm. 2 to be related to the generation of this phase.

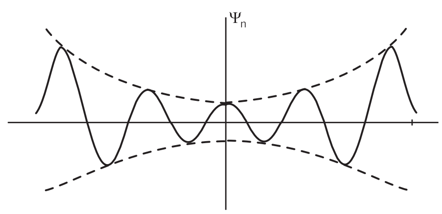

FIGURE 7. Schematic graph of an oscillatory eigenfunction Ψ_n.

4. The Proofs

4.1. **Proof of Theorem 1.** Consider (24), (27)

$$\begin{cases} \dfrac{d^2R}{ds^2} = 2R\big[aR^2 - bms\big], \quad s \in \mathbb{R} \\ R(s) = O(e^s),\ s \to -\infty, \quad \dfrac{R(s)}{\sqrt{\dfrac{bm}{a}s}} = 1 + O\left(\dfrac{1}{s}\right),\ s \to +\infty. \end{cases} \tag{34}$$

We will obtain existence for (34) by the method of sub and supersolutions.

4.1.1. *The subsolution.* We will show the existence of constants $C, d, \lambda > 1$, and a function $g(s)$ with the following properties:

(i) g is smooth, vanishing for $s \leq \lambda$, $g'(s) \geq 0$, g changing convexity only at C, and $g(s) = 1$ for $s \geq d$, with $g(C) = \frac{1}{2}$.

(ii) $4\ (C-1)^2 \geq \dfrac{1}{bm - \max\limits_{\mathbb{R}}|g''(s)|} > 0$

(iii) $\dfrac{1}{(\lambda-1)^2} \leq 2mb(3\lambda+1)$.

Verification of (i), (ii), (iii)

Make a first choice of λ, C, d and g as in (i), to be modified later. By fixing λ for the time being and by taking g sufficiently flat, that is spreading out the transition from 0 to 1 (and so modifying our initial choice of C and d) we can satisfy the 2nd inequality in (ii). Next by translating g to the right, that is by increasing λ, C and d, we can satisfy the first inequality in (ii), and also (iii). We also require $C>1$.

Set

$$\underline{w} = g(s)\sqrt{\sigma(s-1)}, \quad \sigma = \frac{bm}{a} \tag{35}$$

Claim 1. *$\underline{w}$ is a subsolution,*

$$\underline{w}'' \geq 2\underline{w}(a\underline{w}^2 - bms), \quad s \in \mathbb{R} \tag{36}$$

Proof of the Claim: We compute

$$\underline{w}'' = g''\sqrt{\sigma(s-1)} + g'\sqrt{\sigma}\ (s-1)^{-\frac{1}{2}} - \frac{1}{4}\sqrt{\sigma}\ (s-1)^{-\frac{3}{2}}\ g, \tag{37}$$

and verify the claim separately for the concave and convex parts of g.

I. *The Concave Region $s \geq C$*

First we obtain a lower bound for $\underline{w}''$. From (37)

$$\underline{w}'' \geq -\max_{\mathbb{R}}|g''|\sqrt{\sigma(s-1)} - \frac{1}{4}\sqrt{\sigma}(s-1)^{-\frac{3}{2}}. \tag{38}$$

Next we obtain an upper bound for $2\underline{w}(a\underline{w}^2 - bms)$. We compute

$$2\underline{w}(a\underline{w}^2 - bms) = 2g\sqrt{\sigma(s-1)}\ (ag^2\sigma(s-1) - bms) \tag{39}$$

$$\begin{aligned} &= 2g\sqrt{\sigma(s-1)}\ (g^2bm(s-1) - bms) \\ &\qquad \text{(after increasing } C \text{ if necessary)} \\ &\leq 2g\sqrt{\sigma(s-1)}\ (-bm) \\ &\leq -bm\sqrt{\sigma(s-1)}. \end{aligned} \tag{40}$$

Thus, for establishing (35) it is sufficient to satisfy the inequality

$$-\max_{\mathbb{R}}|g''|\sqrt{\sigma(s-1)} - \frac{1}{4}\sqrt{\sigma}\ (s-1)^{-\frac{3}{2}} \geq -bm\sqrt{\sigma(s-1)},$$

which will hold if the following holds

$$(bm - \max_{\mathbb{R}}|g''|)\ \sqrt{s-1} \geq \frac{1}{4}(C-1)^{-\frac{3}{2}},$$

which in turn would hold if

$$4\ (C-1)^2 \geq \frac{1}{bm - \max|g''|}, \tag{41}$$

which is condition (ii) above.

II. *The Convex Region* ($\lambda \le s \le C$) Since

$$\underline{w}'' \ge -\frac{1}{4}\sqrt{\sigma}\ (s-1)^{-\frac{3}{2}}g \qquad \text{by (37)},$$

it is sufficient to establish that

$$-\frac{1}{4}\sqrt{\sigma}\ (s-1)^{-\frac{3}{2}}g \ge 2\underline{w}(a\underline{w}^2 - bms)$$
$$\text{(by (39))} \ = 2g\sqrt{\sigma(s-1)}\ (bms(g^2-1) - g^2bm).$$

Canceling out $g\sqrt{\sigma}$ and noting that

$$s(g^2-1) - g^2 1 \le \lambda(g^2-1) - g^2 1 \le -\frac{3\lambda+1}{4} \qquad \left(0 \le g \le \frac{1}{2}\right),$$

we see that it is sufficient to establish that

$$-\frac{1}{4}(s-1)^{-\frac{3}{2}} \ge -\frac{3\lambda+1}{2}\ bm\sqrt{(s-1)}, \qquad \lambda \le s \le C,$$

or equivalently

$$(s-1)^{-2} \le 2mb(3\lambda+1), \qquad \lambda \le s \le C,$$

which holds by (iii) above. The claim is established.

4.1.2. *The supersolution.* Set

$$\bar{v}(s) = \begin{cases} (\kappa)^{\frac{1}{2}}\sqrt{\sigma}e^s, & s \le 0 \\ \sqrt{\sigma}(s+\kappa)^{\frac{1}{2}}, & s \ge 0, \end{cases} \tag{42}$$

with

(iv) $\kappa \ge 1/2$ and $bm(1+\ln(2\kappa)) \ge 1$.

Claim 2. *$\bar{v}$ is a continuous weak supersolution*

$$\bar{v}'' \le 2\bar{v}(a\bar{v}^2 - bms) \quad \text{weakly}, \quad s \in \mathbb{R} \tag{43}$$

and

$$\bar{v} \ge \underline{w}$$

Proof of the Claim: We will verify that $\bar{v}$ satisfies (43) classically for $s \le 0$ and $s \ge 0$ and that at $s = 0$

$$\bar{v}(0-) = \bar{v}(0+), \quad \bar{v}'(0-) \ge \bar{v}'(0+) \tag{44}$$

I. On $s \le 0$, (43) holds if and only if

$$\kappa^{\frac{1}{2}}e^s \le 2\kappa^{\frac{1}{2}}e^s\ (a\kappa\sigma e^{2s} - bms) \Leftrightarrow a\kappa\sigma e^{2s} - bms \ge \frac{1}{2} \tag{45}$$

which holds by (iv) above.

II. For $s \ge 0$, (43) holds since the right hand side is positive and $\bar{v}'' \le 0$.

III. The transmission conditions (44):

Continuity is immediate. Also,

$$\bar{v}'(0-) = (\kappa)^{\frac{1}{2}}\sqrt{\sigma} \geq \frac{1}{2}\sqrt{\sigma}\frac{1}{(\kappa)^{\frac{1}{2}}} = \bar{v}'(0+) \Leftrightarrow \kappa \geq \frac{1}{2}$$

which holds by (iv) above.

IV. $\bar{v} \geq \underline{w}$ on $\mathbb{R}$

Clearly, $\bar{v} \geq \underline{w}$ for $s \leq \lambda$. For $s \geq \lambda$ note that

$$\sqrt{\sigma}(s+\kappa)^{\frac{1}{2}} > [\sigma(s-1)]^{\frac{1}{2}} \geq g(s)[\sigma(s-1)]^{\frac{1}{2}} = \underline{w}.$$

This proves the claim.

4.1.3. *Existence and estimates.* By a well known theorem [Tr] it follows that there is a solution of $(34)_{(i)}$ satisfying

$$\underline{w}(s) \leq R(s) \leq \bar{v}(s), \qquad s \in \mathbb{R}. \tag{46}$$

It follows that

$$\begin{cases} g(s)\sqrt{\dfrac{bm}{a}}\sqrt{s-k} \ \leq R(s) \leq \sqrt{\dfrac{bm}{a}}\sqrt{s+\kappa}, & s \geq 0, \\ 0 \ \leq R(s) \leq (\kappa)^{\frac{1}{2}}\sqrt{\dfrac{bm}{a}}\ e^{s}, & s \leq 0, \end{cases} \tag{47}$$

giving the asymptotic estimates in (34). Notice that (47) implies in particular that R is strictly positive in $(-\infty,\infty)$. Indeed

$$R(s) \geq 0 \quad \text{for all} \quad s \in (-\infty,\infty)$$

and if $R(s_0) = 0$ for some s_0, then $R'(s_0) = 0$, and therefore by uniqueness R is identically zero.

4.1.4. *The monotonicity.* Finally, we verify the monotonicity of $R(s)$. Since R is strictly positive, (34) implies

$$\left(\frac{R''}{2R} - aR^2\right)' = -bm,$$

i.e.,

$$u'' - \frac{1}{R}uu' - 4aR^2u = -2bm\ R, \tag{48}$$

where

$$u = R'.$$

From the lower bound in (47) it follows by a concavity argument that if $u = R'$ is not strictly positive, then there exists s_0 such that

$$u(s_0) \leq 0,\ u'(s_0) = 0,\ u''(s_0) \geq 0$$

but this is impossible because (48) implies

$$u''(s_0) - 4aR^2u(s_0) = -2bmR(s_0) < 0$$

and therefore we conclude that R' is strictly positive.

The proof of Theorem 1 is complete. □

4.2. **Proof of Theorem 2.** Equation (26) with the asymptotic conditions (27) leads naturally to Airy's equation. We remind the reader of the relevant facts:

The Airy equation is

$$y''(x) = xy(x) \tag{49}$$

The Airy function is the unique (up to a multiple) solution to this equation that decays as $x \to +\infty$. It is denoted by $\mathrm{Ai}(x)$. It satisfies the following asymptotics:

$$\mathrm{Ai}(x) \sim \frac{1}{2}\pi^{-\frac{1}{2}}x^{-\frac{1}{4}}e^{-2x^{\frac{3}{2}}}, \quad x \to +\infty, \tag{50}$$

while $\mathrm{Ai}(x)$ oscillates for $x < 0$ and has all its zeroes in $x < 0$: Its behavior for x negative very closely resembles

$$\pi^{-\frac{1}{2}}(-x)^{-\frac{1}{4}}\sin\left[\frac{2}{3}(-x)^{\frac{3}{2}} + \frac{1}{4}\pi\right] \tag{51}$$

as $x \to -\infty$.

We now return to (26). First from (27) we see that the potential in (26), $q(s) = 2[3aR^2(s) - bms]$, satisfies $\lim_{|s|\to\infty} q(s) = \infty$. From this it follows (see for example [HS] and Theorem XIII.67 in [RS]) that the spectrum of (26) in $L^2(\mathbb{R})$ is discrete with $\lim_{n\to\infty}\mu_n = \infty$. Next we will be applying well-known WKB asymptotics to (26).

4.2.1. *The turning points.* The first step is to check that the equation

$$q(s) - \mu_n = 0, \tag{52}$$

for n large, has exactly two simple solutions. Since $\mu_n \to \infty$, this will follow from showing that $q(s)$ is strictly increasing (decreasing) for $s > B$ ($s < -B$), B appropriately large and fixed.

We have that

$$\frac{1}{2}q'(s) = 6aR(s)R'(s) - bm. \tag{53}$$

<u>The case $s \to \infty$.</u>

We will establish the estimate

$$R'(s) > As^{-1/2}, \; s > B, \tag{54}$$

where A is any number satisfying

$$A < \frac{1}{2}\sqrt{bm/a}, \tag{55}$$

and B depends on A.

Then by (53), (27), and (55),

$$\frac{1}{2}q'(s) = 6aR(s)R'(s) - bm = 6a\sqrt{\frac{bm}{a}}s\,(1 + o(1))R'(s) - bm$$

$$> 6a\sqrt{\frac{bm}{a}s}\,(1+o(1))As^{-1/2} - bm$$
$$= 6\sqrt{abm}A(1+o(1)) - bm,$$

which can be made arbitarily close to $3bm(1+o(1)) - bm$, from which it follows that $q'(s) > 2bm > 0,\ s > B > 0$. Thus q is strictly increasing for $s > B$.

Proof of (54). In the following, A will be a fixed number satisfying (55). We will be working with Eq. (48):

$$u'' - \frac{1}{R}uu' - 4aR^2u = -2bmR,\ u \equiv R' > 0. \tag{56}$$

We begin by verifying that $\underline{u} = As^{-1/2}$ is a subsolution to (56). By (25) the desired inequality is

$$\frac{3}{4}As^{-5/2} + \frac{1}{2R}A^2s^{-2} - 4a\left\{\sqrt{\frac{bm}{a}s}\,(1+o(1))\right\}^2 As^{-1/2}$$
$$\geq -2bm\sqrt{\frac{bm}{a}s}\,(1+o(1)).$$

For this to hold for large enough s, it is sufficient to show that

$$4a\left(\frac{bm}{a}s\right)(1+o(1))As^{-1/2} < 2bm\sqrt{\frac{bm}{a}s}\,(1+o(1)),$$

which in turn follows from (55).

Next, we indicate briefly how the comparison argument is completed to render (54).

Step I: Show that there is a $B > 0$ such that $\underline{u}_\delta(s) = As^{-1/2} - \delta$ is a strict subsolution of (56) for $s \geq B$, uniformly in $\delta \in [0,1)$. This is done by a routine calculation similar to the above.

Step II: Since $v \equiv 0$ is a subsolution of (56), it follows that $w_\delta(s) = (As^{-1/2} - \delta)^+$ is a strict subsolution of (56) for $s \geq B$.

Step III: Find a number B, depending on A, such that

$$R'(B) = u(B) > AB^{-1/2} \geq w_\delta(B). \tag{57}$$

for all $\delta \in [0,1]$. For integers n, by (27), $R(n) = \sqrt{bm/a}\ n^{1/2}(1 + O(n^{-1})),\ n \to \infty$. Thus

$$R(n+1) - R(n) = \frac{1}{2}\sqrt{bm/a}\ n^{-1/2}(1 + O(n^{-1})).$$

For each n there exists a number $\hat{n} \in (n, n+1)$ such that the left side is $R'(\hat{n})$. It follows that for some α independent of n,

$$R'(\hat{n}) = \frac{1}{2}\sqrt{bm/a}\ \hat{n}^{-1/2}(1 + O(n^{-1})) > \frac{1}{2}\sqrt{bm/a}\ \hat{n}^{-1/2}(1 - \alpha n^{-1}) > A\hat{n}^{-1/2}$$

for large enough n, by (55). The inequality (57) (it suffices to set $\delta = 0$) now follows with $B = \hat{n}$.

Step IV: By taking δ large (say $\delta = \delta_0$) we can guarantee that

$$u(s) > w_{\delta_0}(s), \ s \geq B. \tag{58}$$

Step V: We intend to reduce δ continuously to 0 and show that (58) holds for δ_0 replaced by all $0 < \delta \leq \delta_0$. If (58) were violated at some point in this process, let δ^* be the first value of δ where the violation occurs, and s^* the location. Then by (57), $s^* > B$ and also $s^* < \infty$ (since $u > 0$ and $w_{\delta^*} = 0$ for s large). Therefore

$$u(s^*) = w_{\delta^*}(s^*), \ u'(s^*) = w'_{\delta^*}(s^*), \tag{59}$$

$$u(s) \geq w_{\delta^*}(s), \ s \geq B. \tag{60}$$

Evaluating (56) at $s = s^*$ and utilizing that w_{δ^*} is a strict subsolution, we get

$$w''_{\delta^*}(s^*) - \frac{1}{R(s^*)} w_{\delta^*}(s^*) w'_{\delta^*}(s^*) - 4aR^2(s^*) w_{\delta^*}(s^*) > -2bmR(s^*),$$

and conclude via (59) that $w''_{\delta^*}(s^*) - u''(s^*) > 0$, which contradicts (60) in a right neighborhood of s^* (via (59)). Thus we can take $\delta \to 0$ and obtain (54).

The case $s \to -\infty$.

This is very easy compared to the previous case. From (24) it follows that $R'' > 0$ for $s < 0$. Thus R' is increasing. This, together with (27), shows that $R(s)R'(s) \to 0$ as $s \to -\infty$. Consequently from (53) we see that $q'(s) < 0$ for $s < -B$.

In conclusion, we established that

$$\mu_n - 2(3aR^2(s) - bms) = 0 \tag{61}$$

has two simple solutions $A_n < 0 < B_n$, for n large. We now apply the results of WKB asymptotic analysis (see e.g. [BO] p. 521, especially the example) to conclude that

$$\int_{A_n}^{B_n} \sqrt{\mu_n - 2(3aR^2(s) - bms)}\, ds = (n + \frac{1}{2})\pi + O(1), \ n \to \infty;$$

$[A_n, B_n]$ is the oscillatory range of the nth eigenfunction.

4.2.2. *Further properties.* From (47) and (61) via (27) we obtain after a few calculations the asymptotic relations

$$\begin{aligned} &A_n \sim -\tfrac{\mu_n}{2bm}, \qquad B_n \sim \tfrac{\mu_n}{4bm}, \\ &\mu_n \sim \left[2bm\left(n + \tfrac{1}{2}\right)\pi\right]^{\frac{2}{3}} \end{aligned} \tag{62}$$

Utilizing once more the asymptotics (27), we note that for s outside a fixed large interval $[-K, K]$, $K > 0$, the eigenfunctions V_n approximately satisfy the equation

$$y'' - [4bms - \mu]y = 0, \qquad s \geq K,$$

$$y'' - [-2bms - \mu]y = 0, \qquad s \leq -K.$$

Thus

(63)

$$\begin{cases} V_n(s) \text{ is approximated by } c_n \mathrm{Ai}\Big((4bm)^{\frac{1}{2}}\Big(s-\dfrac{\mu_n}{4bm}\Big)\Big), \text{ for } s \geq K, \text{uniformly in } n, \\ V_n(s) \text{ is approximated by } d_n \mathrm{Ai}\Big((2bm)^{\frac{1}{2}}\Big(-s-\dfrac{\mu_n}{2bm}\Big)\Big), \text{ for } s \leq -K, \text{uniformly in } n, \end{cases}$$

where c_n and d_n are constants to be estimated from the normalization. Indeed using (62), (63), (50), and (51), we obtain that c_n and d_n are $O\left(n^{-1/6}\right)$. The calculation that gives this takes into account the ever increasing number of oscillations outside the fixed interval $[-K, K]$ as n increases, and employs the asymptotic estimates (50) and (51).

By Sturmian theory the eigenvalues μ_n are simple and their corresponding eigenfunctions have exactly $n-1$ nodes.

Finally, we show that the principal eigenvalue is positive,

$$\mu_1 > 0. \tag{64}$$

We argue by contradiction. Assume that $\mu_1 \leq 0$. Since V_1 is the principal eigenfunction it can be chosen so that $V_1 > 0$, and therefore it satisfies

$$V_1'' - 2[3aR^2(s) - bms]V_1 = -\mu_1 V_1 \geq 0, \qquad \text{on } \mathbb{R}, V_1 \in L^2. \tag{65}$$

Thus V_1 is a positive subsolution of the operator defined by the left side of (65).

Utilizing the asymptotics in (27) by a comparison argument we obtain, via (50), the estimate

$$0 < V_1(s) \leq C_1 e^{-C_2|s|^{\frac{3}{2}}} \tag{66}$$

for appropriate constants C_1, C_2. From (65), via (66) and a standard argument, similar estimates hold for the derivative of V_1,

$$|V_1'(s)| \leq C_1 e^{-C_2|s|^{\frac{3}{2}}}. \tag{67}$$

We note that the specific exponent is not important here. All that matters is the integrability on all $\mathbb{R}$ of the estimating function.

Differentiating (34) and setting $w = \frac{dR}{ds}$ we obtain

$$w'' - 2[3aR^2(s) - bms]w = -2bmR(s) < 0. \tag{68}$$

By Theorem 1, $w > 0$. Multiplying (65) by w and (68) by $-V_1$ and adding, we obtain

$$wV_1'' - w''V_1 > 0 \Longleftrightarrow (wV_1' - w'V_1)' > 0. \tag{69}$$

By (66), (67) and simple estimates on R', R'' we have that

$$\lim_{s\to-\infty}(wV_1' - w'V_1) = 0$$

Hence, by (69)

$$wV_1' - w'V_1 > 0 \Longleftrightarrow \frac{w'}{w} < \frac{V_1'}{V_1}.$$

Integrating we obtain

$$\int_{s_0}^{s} \frac{w'}{w} ds < \int_{s_0}^{s} \frac{V_1'}{V_1} ds \Longleftrightarrow \ln\left(\frac{w(s)}{w(s_0)}\right) < \ln\left(\frac{V_1(s)}{V_1(s_0)}\right)$$

or

$$0 \le w(s) < cV_1(s), \quad c \quad \text{a constant},$$

i.e.,

$$0 \le R'(s) < cV_1(s), \;\; s \in I\!R. \tag{70}$$

From the estimate $R(s) = O(e^s)$ as $s \to -\infty$ and (70) it follows that

$$\begin{aligned} 0 \le R(s) \;\; &= \;\; \int_{-\infty}^{s} R(s)ds < c\int_{-\infty}^{s} V_1(s)ds \\ \text{(by (66))} \;\; &\le \;\; c\int_{-\infty}^{s} e^{-c|s|^{\frac{3}{2}}} ds \le C, \quad \text{uniformly in } s. \end{aligned} \tag{71}$$

Estimate (71) contradicts (27).

The proof of Theorem 2 is complete. □

ACKNOWLEDGMENTS

We would like to thank G. Karali for her help during the preparation of the paper. We would also like to thank V. Papanicolaou for a useful discussion on the spectral problem.

References

[AFFS] N.D. Alikakos, P. Fife, G. Fusco and C. Sourdis, Analysis of the heteroclinic connection of a singularly perturbed problem, preprint.

[AMP] S.B. Angenent, J. Mallet-Paret and L.A. Peletier, Stable transition layers in a semilinear boundary value problem, *Journal of Differential Equations* **67** (1987), 212–242.

[BCMcFW] R.J. Braun, J.W. Cahn, G.B. McFadden, and A.A. Wheeler, Anisotropy of interfaces in an ordered alloy: a multiple-order-parameter model, *Trans. Roy. Soc. London* A 355 (1997), 1787.

[BO] C.M. Bender and S.A. Orszag, Advanced Mathematical Methods for Scientists and Engineers, Asymptotic Methods and Perturbation Theory, Springer, 1999.

[CMcF] S.R. Coriell and G.B. McFadden, Morphological Stability, in *Handbook of Crystal Growth*, D.T.J. Hurle ed., Elsevier-North Holland, Amsterdam (1993), 785-857.

[DS] N. Dunford and J.J. Schwartz, Linear Operators Part II, Interscience, New York, 1963.

[Fe] N. Fenichel, Geometric singular perturbation theory for ordinary differential equations, *J. Differential Equations* **31**, 55–98 (1979).

[G] M.E. Gurtin, Thermomechanics of Evolving Phase Boundaries in the Plane, *Oxford Math. Monographs*, Clarendon Press, 1993.

[HS] P. Hislop and I. M. Sigal, Introduction to Spectral Theory with Applications to Schrödinger Operators, Applied Mathematics Sciences, Volume 113, Springer-Verlag, New York, 1996.

[HC] D.W. Hoffman and J.W. Cahn, A vector thermodynamics for anisotropic surfaces: I. Fundamentals and application to plane surface junctions, *Surface Science* **31** (1972), 368.

[J] C. K. R. T. Jones, Geometric singular perturbation theory, pp. 44–118 in L. Arnold, C. Jones, K. Mischaikow and G. Raugel, Dynamical Systems, Lecture Notes in Mathematics **1609**, Springer-Verlag, 1995.

[KC] R. Kikuchi and J.W. Cahn, Theory of interphase and antiphase boundaries in FCC alloys, *Acta Metall.* **27** (1979), 1337.

[Ni] Y. Nishiura, Mathematics of Patterns, Monograph, to be published by AMS.

[NC] A. Novick-Cohen and J. W. Cahn, Evolution equations for phase separation and ordering in binary alloys, *J. Stat. Phys.* **76** (1994) 877–909.

[PE] D.A. Porter and K.E. Easterling, Phase Transformations in Metals and Alloys, 2nd edition, Chapman and Hall.

[RS] M. Reed and B. Simon, Methods of Modern Mathematical Physics, Vol. IV, Academic Press, 1978.

[S] C. Sourdis, Master thesis, University of Athens, 2003.

[T] G.B. Tanoglu, Ph.D. Thesis, University of Delaware, Dept. Appl. Math., 2000.

[TBCMcF] G. B. Tanoglu, R.J. Braun, J.W. Cahn, and G. B. McFadden, $A1 - L1_0$ phase boundaries and anisotropy via multiple-order-parameter theory for an FCC alloy, *Interfaces and Free Boundaries* **5** (2003), 275-299.

[Tr] F. Treves, Linear partial differential equations with constant coefficients: Existence, approximation and regularity of solutions, Mathematics and its Applications, Vol. 6, Gordon and Breach Science Publishers, New York-London-Paris, 1966.

N.D. Alikakos, Department of Mathematics, University of North Texas and University of Athens
E-mail address: `nalikako@earthlink.net`

P.W. Bates, Department of Mathematics, Michigan State University, East Lansing, MI 48824
E-mail address: `bates@math.msu.edu`

J.W. Cahn, Division of Material Science, N.I.S.T.
E-mail address: `john.cahn@nist.gov`

P.C. Fife, Department of Mathematics, University of Utah, UT 84112
E-mail address: `fife@math.utah.edu`

G. Fusco, Univ. degli Studi dell'Aquila
E-mail address: `fusco@mailhost.univaq.it`

G.B. Tanoglu, Department of Mathematics, Izmir Institute of Technology
E-mail address: `gtanoglu@likya.iyte.edu.tr`